Anal. Chem. **1996,** *68,* 2758−2765

Acoustic Flame Detector for Gas Chromatography

Kevin B. Thurbide, Peter D. Wentzell, and Walter A. Aue*

Trace Analysis Research Centre, Department of Chemistry, Dalhousie University, Halifax, NS, Canada B3H 4J3

A novel gas chromatography detector is described that uses acoustic signals from a partly premixed hydrogen−air flame burning on top of a capillary. The device, referred to as the acoustic flame detector (AFD), is based on the measurement of the frequency of acoustic transients generated at the burner under a range of operating conditions. The presence of trace amounts of analyte in the flame was found to increase the frequency of these sonic bursts from the baseline level of ∼100 Hz. The response of the AFD for *n*-dodecane, measured as the shift in frequency, was determined to be linear over ∼3 orders of magnitude, with a minimum detectable level of about 1−5 ng C/s using the current system. The sensitivity correlates roughly with carbon content, except for certain organometallics (Sn, Mn), which gave substantially enhanced signals. Some tailing was observed but became serious only for particular types of organometallics. The noise of the system was predominantly of the 1/*f* type. The effects of flow conditions, burner geometry, and flame gas constituents were investigated. The oscillations could be followed by acoustic, visual, electrical, and optical means. The AFD mechanism is shown to involve oscillatory chemical kinetics, in which the flame front (the inner cone) temporarily enters a few millimeters into the capillary during each cycle, thereby creating the acoustic signal.

Gas chromatography (GC) has long been one of the most important instrumental techniques in analytical chemistry, and GC detectors have been developed that are based on almost every conceivable physical measurement.[1−4] Commonly used detectors are based on measurements of the thermal, electrical, spectral, and chemical characteristics of the eluent. The variety of detectors available, both selective and universal, is a consequence of the breadth of areas to which GC has been applied. This paper describes a completely novel GC detection method that is based on acoustic measurements.

In recent years, the analytical applications of acoustic measurements have gained greater attention. These include what can be called "active" acoustic methods, such as photoacoustic spectroscopy and surface acoustic wave methods, as well as "passive" methods, where no controlled source of acoustic modulation is used. While the successes in the former category are well documented, the development of passive acoustic methods in analytical chemistry has been largely restricted to qualitative applications.[5] Quantitative applications have been limited by the fact that acoustic events are essentially macroscopic phenomena, requiring relatively large numbers of analyte molecules for a substantial signal to be generated. As a result, limits of detection are typically high. Nevertheless, Wentzell et al. were the first to demonstrate that quantitative measurements could be performed with passive acoustic emission through the development of a hydrogen peroxide sensor based on catalytically generated effervescence.[6] Although detection limits were too high for practical use, the principles of this method were later used to develop a flow-injection method for carbonate based on acoustic emission.[7] The present development is a departure from these solution methods and is based on subtle modifications to flame chemistry brought about by the presence of an analyte. Although this method does not rival the sensitivity of traditional GC detectors such as the flame ionization detector (FID), it represents a tremendous advance in the sensitivity of passive acoustic sensors. Furthermore, it may provide an alternative approach to the study of flame-based detectors and offer as yet unforeseen advantages for GC analysis.

The development of the acoustic flame detector (AFD) resulted from an investigation of the reactive flow detector (RFD), recently described by Thurbide and Aue.[8,9] In simple terms, the RFD consists of a capillary in which a reactive flow (a luminescent column of hydrogen-rich, H_2−air premix) is established with optical characteristics similar but not identical to those of a conventional flame photometric detector (FPD). When a solvent peak enters the RFD, the reactive flow is temporarily expelled from the capillary. It then relights on the coexisting air-rich flame burning atop the capillary. This process is accompanied by characteristic sounds that change markedly in pitch and intensity, allowing the operator to "hear" the solvent peak. Further investigation showed that, if the air flow in the capillary is adjusted to a value just short of the stability range of the reactive flow, the flame burning on top of the capillary will emit a steady and clearly audible acoustic signal. The frequency of this signal remains constant for a given set of conditions but will change when analytes (or the solvent) elute from the column and pass through the flame. This change in pitch suggests that the device might serve as an acoustic detector for GC.[9]

Flame noise in general and flame oscillations in particular have long been a subject of intense interest in science and technology. Considerable research from diverse fields has defined and

(1) Adlard, E. R. *Crit. Rev. Anal. Chem.* **1975**, *5*, 1−36.
(2) Dressler, M. *Selective Gas Chromatography Detectors*; Journal of Chromatography Library 36; Elsevier: Amsterdam, 1986.
(3) McMinn, D. G.; Hill, H. H. *Detectors for Capillary Chromatography*; Chemical Analysis Series 121; Wiley: New York, 1992; Chapter 2.
(4) Poole, C. F.; Schuette, S. A. *Contemporary Practice of Chromatography*; Elsevier: Amsterdam, 1984.
(5) Wade, A. P.; Sibbald, D. B.; Bailey, M. N.; Belchamber, R. M.; Bittman, S.; McLean, J. A.; Wentzell, P. D. *Anal. Chem.* **1991**, *63*, 497A−507A.
(6) Wentzell, P. D.; Vanslyke, S. J.; Bateman, K. P. *Anal. Chim. Acta* **1991**, *246*, 43−53.
(7) Little, M. J.; Wentzell, P. D. *Anal. Chim. Acta* **1995**, *309*, 283−292.
(8) Thurbide, K. B.; Aue, W. A. *J. Chromatogr.* **1994**, *684*, 259−268.
(9) Thurbide, K. B. Ph.D. Thesis, Dalhousie University, Halifax, NS, Canada, 1994.

S0003-2700(95)01243-1 CCC: $12.00

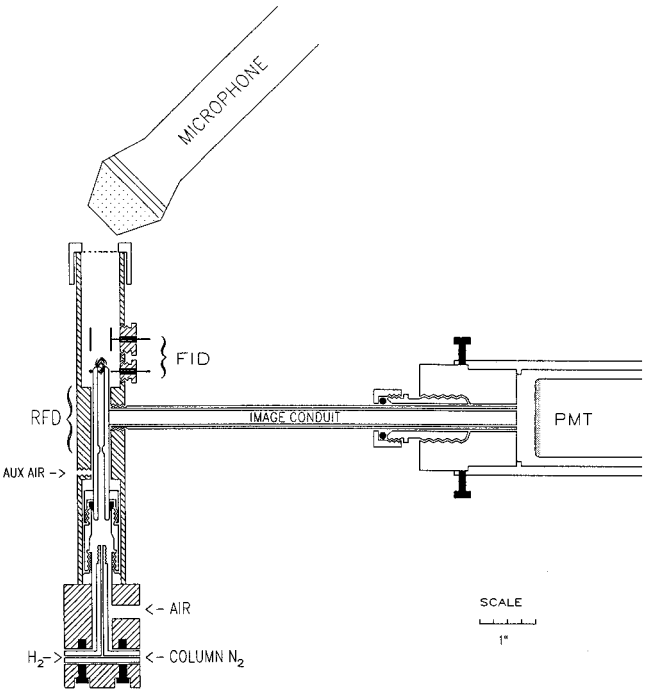

Figure 1. Schematic diagram of acoustic flame detector, with flame ionization and photometric detection components also shown.

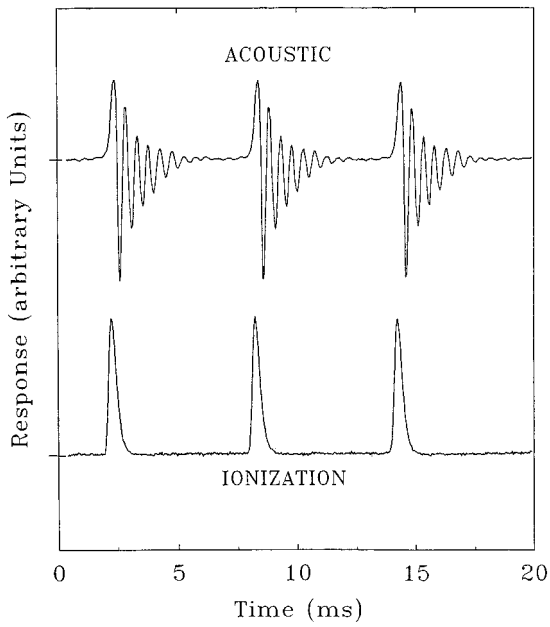

Figure 2. Comparison of acoustic and flame ionization detector signals in the presence of analyte. The tic marks on the left-hand axis denote the baseline response for each signal.

sometimes even explained the workings of different types of oscillatory combustion systems.[10] In gas chromatography, an FID based on a "singing flame" has produced ion yields 2−3 times higher than a conventional FID.[11] In other cases, flame oscillations have been considered more of a nuisance.[12] Farther afield, frequency changes of an oscillating glow discharge plasma in the 10^5-10^6 Hz region have been used for gas chromatographic detection.[13,14]

The objective of this study was to develop and characterize the acoustic flame detector. The instrumentation and conditions needed to induce the acoustic signal are described, and the response characteristics of this novel mode of detection are examined.

EXPERIMENTAL SECTION

The AFD used the same chromatographic system and detector housing as the previously described RFD,[8] shown in Figure 1. The configuration also permitted detection by a conventional FID and photometric monitoring of the signal. For operation as an AFD, the air flow was adjusted such that a steady oscillation was obtained in the air-rich flame atop the capillary. Typical operating conditions using a 1.8 mm i.d. capillary consisted of a premix of air and hydrogen at 45 mL/min each and a column nitrogen flow of 12 mL/min. The flame on top of the capillary was made air-rich—and thereby maintained at all conditions—by an external auxiliary air flow of ~70 mL/min. The oscillatory flame behavior was generally easy to hear and, depending on the burner design, could be maintained with good stability over a fairly wide range of conditions. Several different capillary diameters and designs were investigated in this work, and, while there were some changes in response characteristics (e.g., baseline frequency, sensitivity), comparable results were generally obtained with all configurations.

Other than adjustment of the flow rates, the only modification necessary to convert the RFD into the AFD was the addition of an inexpensive external microphone (Realistic Model 33-986B) and associated electronics. A metal screen was also placed on top of the detector housing to reduce the effect of air currents in the room. The microphone was connected to the input of an amplifier (Bruel and Kjaer Model 2638, Naerum, Denmark) with a low-pass filter set at 10 kHz. A digital storage oscilloscope (Tektronix Model 2232, Beaverton, OR) was used to monitor the amplifier output, which was also fed to a burst detect circuit that has been previously described.[6] This circuit was designed to provide a TTL pulse for every acoustic burst occuring at the microphone. To do this, a comparator triggered a monostable multivibrator at the onset of the acoustic burst. The pulse length of the monostable was set to 750 μs, sufficiently long so that it would be retriggered by oscillations in an extended acoustic burst, thereby avoiding multiple detection of a single burst. The TTL output of the burst detect circuit was connected to a binary input of an IBM data acquisition and control adapter (DACA), which was housed in a PC-AT computer. The 8253 timer/counter of the DACA was used to measure the time between rising edges of the TTL output of the burst detect circuit, thereby providing the time interval between acoustic bursts with a resolution of 10 μs. These time intervals were ultimately converted to frequencies.

RESULTS AND DISCUSSION

Signal Characteristics. Figure 2 shows a typical acoustic signal obtained on the oscilloscope when analyte is passing through the AFD. For comparison, the signal from the FID is also shown. The acoustic signal consisted of a series of regularly spaced bursts, each burst represented by an exponentially damped sinusoid characteristic of a transient acoustic event. It was found that the magnitude of the acoustic signal (i.e., the maximum

(10) Gaydon, A. G.; Wolfhard, H. G. *Flames*; Wiley: New York, 1979.
(11) Graiff, L. B. *Nature* **1964**, *203*, 856.
(12) Hill, H. H.; Aue, W. A. *J. Chromatogr. Sci.* **1974**, *12*, 541−545.
(13) Kuzuya, M.; Piepmeier, E. H. *Anal. Chem.* **1991**, *63*, 1763−1766.
(14) Smith, D. L.; Piepmeier, E. H. *Anal. Chem.* **1994**, *66*, 1323−1329.

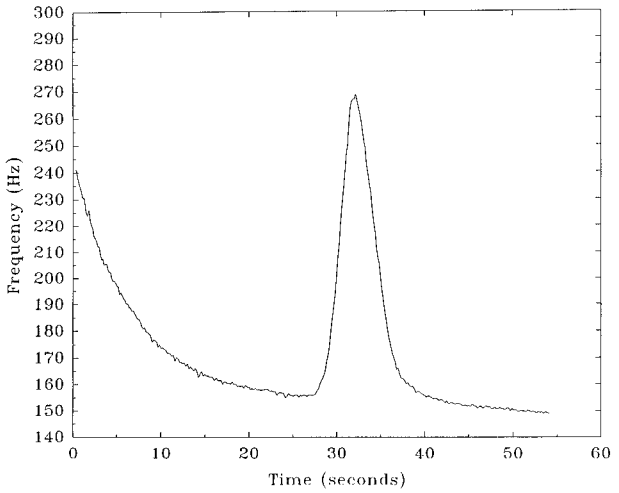

Figure 3. Acoustochromatogram for *n*-dodecane (20 μg, isothermal run at 200 °C).

amplitude of the burst) was essentially independent of the amount of analyte present, as was the frequency of the sinusoidal oscillations within each burst, but the time between bursts generally decreased as the amount of analyte was increased. This change in pitch was clearly audible when the concentration of analyte was relatively high. At a limit of very high concentration (e.g., the solvent front), the oscillations would stop altogether but then spontaneously resume when the concentration of the hydrocarbon dropped to a suitable level. The baseline frequency of the bursts was typically around 100 Hz, and, although this could be modified somewhat by changing the burner design or operating conditions, it was quite stable for a given set of conditions.

Because of the apparent dependence of the frequency of the acoustic bursts on concentration, the chromatographic response of the AFD was investigated. Figure 3 shows a typical "acoustochromatogram" (or "phonogram") for *n*-dodecane, in which the frequency of the acoustic bursts is plotted against time. The large signal decrease at the left side is due to the tail of the solvent peak. For the most part, the shape of the analyte peak is typical of a chromatographic response, although signals from the AFD seem to show a significantly greater amount of tailing than other detection modes, thus possibly implying some memory effect.

Mechanistic Observations and Interpretation. Figure 2 indicates that the acoustic signals from the AFD were transient in nature, in contrast to the behavior of conventional "singing" flames. The latter depend on physical resonance processes within the burner that lead to sinusoidal oscillations with a characteristic "organ pipe" frequency. Furthermore, the baseline frequency of the AFD was much lower than that of typical singing flames and did not depend on the length of the capillary as would be expected for burner resonance. Similarly, clamping the capillary in various places had no effect on frequency. Even the "ringing" frequency of each sonic burst seemed unrelated to burner geometry. When a piezoelectric transducer was directly mounted on the assembly, acoustic coupling was quite poor. These experiments suggest that the acoustic transient is not dependent on, nor is it efficiently coupled to, the detector assembly. To further ensure that the effect of analyte on the oscillatory behavior of the flame was not simply a bulk effect related to a modification of the composition of the flame gases, the contribution of the analyte to the premixed gases was calculated. At the upper end of the detection range, the amount of dodecane represents about 0.03% by volume of the premixed gases, a level which should be much too small to significantly modify flame stoichiometry. This supports a speculative interpretation of the AFD's mechanism as one primarily ruled by oscillatory chemical kinetics as opposed to physical resonance. The presence of hydrocarbons in the mixture is likely to slow down reaction kinetics and decrease the burning velocity of the flame. It is felt that this is the ultimate factor influencing the frequency of the oscillations.

Additional evidence of a transient event is provided by monitoring ionization in a flame doped with a small amount of analyte. The FID signal, shown in Figure 2, is a sharp, unipolar pulse coincident with the maximum of the acoustic burst. (Although a time difference might be expected due to the fact that electron collection is faster than the speed of sound, calculations indicate that this difference would be <1 ms.) Within the limits of oscillographic resolution, this electrical pulse contains all of the charge collected per oscillation. Consequently, in the absence of analyte, the FID pulse drops to near baseline level. The presence of a single sharp pulse could indicate that it is the flame front that oxidizes most or all of the carbon available within a given cycle.

The oscillations of a typical AFD are too fast to be resolved by the naked eye, but averaged spatial effects could still be readily observed. In all instances, the flame appeared to burn continuously with no evidence of extinction and reignition, even when the solvent passed through. In the absence of analyte, the flame consisted of an inner and outer cone, the inner cone extending from roughly 1 mm above the capillary to about 1 mm inside the capillary. It should be noted that these observations were made with the detector housing removed and only ambient air supporting the outer parts of the flame. Inside the detector, air flow provided by an auxiliary supply is somewhat restricted, resulting in a slightly lower frequency of the oscillating flame. Consequently, the flame front excursion into the the capillary is expected to be >1 mm under normal AFD operating conditions.

As the amount of analyte (or solvent) in the flame increases, the bottom of the inner cone starts to withdraw from the inside of the capillary and eventually becomes level with the top of the burner. In the presence of substantial amounts of solvent, the top of the inner cone extends well into the body of the flame, and audible oscillations terminate.

It should be noted that the flow conditions for stable acoustic emission from the air-rich flame on top of the capillary in the AFD mode are close to the regime of stable optical emission from the hydrogen-rich luminescent column filling the capillary in the RFD. Thus, the inner cone of the AFD flame extends some distance into the capillary but not enough to descend to the quenching restriction and form a reactive flow. An increase in the flow of premix air, in fact, will establish the reactive flow.

To allow a visual observation of the oscillations in the AFD, and to improve the definition of the flame dynamics, the flame image was modulated with an eight-blade chopper wheel (1:7 duty cycle) matched to the prevailing frequency. The flame was illuminated with small amounts of an organophosphate, and flow conditions were adjusted to yield maximum spatial change. When viewed through the chopper wheel, the flame appeared to pulsate asymmetrically (i.e., with different speeds moving into and out of the capillary). The HPO* emission was strong enough to permit extended-exposure photographs to be taken. Three of these, showing relevant stages of oscillation, are reproduced in Figure

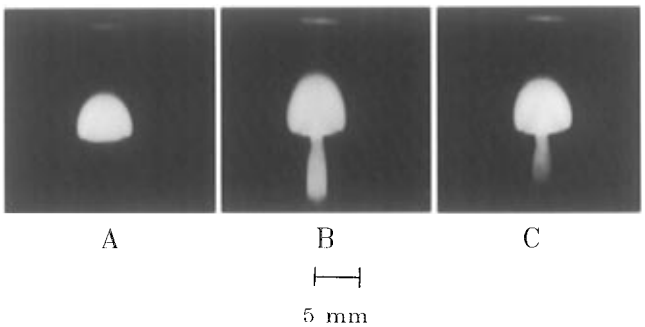

Figure 4. Time-resolved photographs of oscillating flame. The first two frames show the limits of flame front travel within the capillary; the last frame shows an intermediate stage.

4. These show clearly the limits of the oscillatory motion of the flame and the extent of the excursion into the capillary. The photograph on the left represents the flame at its smallest volume. The roughly hemispherical luminescence rests on top of the capillary and shows no evidence of a reaction occurring inside. The entry of auxiliary air across the rim can be seen as darker areas owing to the lower temperature and higher oxygen content. As the oscillation takes place, the flame on top of the burner moves into the capillary and then retreats once more. The size of the luminescent volume, both above and below the rim of the capillary, displays a faster increase than decrease. It is believed that the rapid movement of the flame front down the capillary leads to the transient pressure wave giving rise to the acoustic signal. The photograph in the middle shows the flame at its greatest extension. The luminescence has descended about 7.6 mm into the capillary, and the flame on top of the capillary has increased in volume. (Note that the pinched appearance at the top of the capillary is due to firepolishing and appears larger than it actually is because of the magnification by the capillary.) The photograph on the right shows the flame as it decreases in size. The luminescent column at this point is shorter and weaker and continues to diminish until it again reaches the state represented by the photograph on the left. It should be pointed out that the nature of the reaction causing HPO chemiluminescence is not securely established.[15,16] Furthermore, this emission is delayed by about 2 ms relative to that of OH or CH[17,18] and is strongly dependent on temperature and flame composition. Caution must therefore be exercised when equating the boundary of the luminescence with that of the flame, as the two may not exactly coincide.

Figure 4 confirms that a temporary flame front travels a significant distance inside the capillary. This is not surprising since, if given a slightly increased air flow, the front would travel all the way to the bottom restriction and establish a permanent, nonoscillating, reactive flow throughout the capillary (as in the RFD). The hydrogen-rich inner cone of the flame on top of the capillary contains a large concentration of free radicals, such as the propagating H atom. These species allow a premixed flame front to move downward into the unburnt stream of gas, shielded only by a preheating zone. Flashback is an example of this phenomenon and is commonly studied in combustion tubes.

Flashback does not occur in a tube whose diameter is smaller than the so-called quenching diameter. Quenching diameters for common hydrogen−air flames are ∼0.5 mm. They are believed to be determined by efficient H atom removal through the surface reaction:[10]

$$H^{\bullet} + O_2 \rightarrow HO_2^{\bullet} \qquad (1)$$

While quenching diameters are known to be affected by temperature, they are much more strongly influenced by the burning velocity. Essentially, the faster the burning velocity of the premix, the smaller the quenching diameter required to terminate propagation of the flame front.

Burning velocities of hydrogen−air flames are considerably larger than those of most hydrocarbon−air systems but are, of course, still not as large as those of the well studied hydrogen−oxygen reaction. The magnitude of the burning velocity depends on the "strength" of the premixture. As increasing amounts of air are introduced into the fuel, the burning velocity will tend to rise but will usually achieve a maximum value within the fuel-rich region. For hydrogen−air flames, the greatest burning velocity is observed for oxygen concentrations that are about one-half of the elemental stoichiometry of water.[10]

It is well known that the burning velocity of hydrogen−air flames is greatly reduced in the presence of a small percentage of hydrocarbon additive.[10,19] This should not be confused with an effect on the mixture strength, which would also change the burning velocity, but only if much larger quantities of hydrocarbon were involved. The measured decrease is assumed to arise from the capture of the key propagating species, H•, through reactions such as

$$H^{\bullet} + CH_4 \rightarrow H_2 + {}^{\bullet}CH_3 \qquad (2)$$

Variations on this theme also exist for olefins, halogens, etc., but they all have in common the removal of H•. A similar situation may exist in the quenching of some flame photometric responses.[20,21] The burning velocity has also been shown to vary linearly with the concentration of H atoms for a number of systems, including hydrogen−oxygen flames.[10]

For the typical AFD oscillating flame, premix oxygen is introduced at about 40% of the amount required by stoichiometry. This is slightly lower than the level at which maximum burning velocity is obtained (about 54%). (Larger oxygen concentrations will establish a reactive flow and, at levels above 50% of stoichiometric, will even collapse the reactive flow into a second, hydrogen-rich flame burning at the lower restriction.[8]) The burning velocity of a flame combusting a premix of the same composition as that used in the AFD is estimated at ∼225 cm s^{-1}.[10,19] This contrasts with the premix gas velocity through the capillary of ∼67 cm s^{-1} at room temperature and pressure (or ∼140 cm s^{-1} at 350 °C).

As the flame front travels into the capillary, it uses up most or all of the oxygen contained in the premix column. Since the reaction is highly exothermic, the gas temperature rises rapidly,

(15) Gilbert, P. T. In *Analytical Flame Spectroscopy*; Mavrodineanu, R., Ed.; MacMillan: London, 1970; Chapter 5.
(16) Syty, A.; Dean, J. A. *Appl. Opt.* **1968**, *7*, 1331−1336.
(17) Atar, E.; Cheskis, S.; Amirav, A. *Anal. Chem.* **1991**, *63*, 2061−2064.
(18) Cheskis, S.; Atar, E.; Amirav, A. *Anal. Chem.* **1993**, *65*, 539−555.
(19) Miller, D. R.; Evers, R. L.; Skinner, G. B. *Combust. Flame* **1963**, *7*, 137−142.
(20) Aue, W. A.; Sun, X. Y. *J. Chromatogr.* **1993**, *641*, 291−299.
(21) Thurbide, K. B.; Aue, W. A. *J. Chromatogr.* **1995**, *694*, 433−440.

and the resultant pressure wave is observed as the primary acoustic transient. Movement of the flame front is arrested by the diminishing supply of radicals resulting from the decrease in density of the suddenly heated fuel mixture and encounters with the capillary wall. The reaction temporarily ceases at this point until fresh premix flow again fills that part of the capillary. Meanwhile, only residual hydrogen is supplied to the flame. Since the rate of movement of the flame front down the capillary is greater than the gas velocity traveling upward, more time is needed to refill the capillary with the combustible mixture. After this period, the gas mixture in the capillary is reignited by the flame, and the next flame front moves down the capillary. It is not entirely clear when this reignition occurs, but some volume of premixed fuel may have to enter the flame. The difference between the largest and the smallest flame sizes in the photograph may shed some light on this effect, although the volume changes caused by the fluctuating temperature and pressure make an accurate interpretation difficult.

The scenario presented above can be buttressed by some simple calculations. The photographs of Figure 4 show the flame front igniting the combustible mixture about 7.6 mm deep into the capillary. To do this, the flame front requires about 3.4 ms at an estimated burning velocity of 225 cm s^{-1}.[10] It will take fresh premix about 5.4 ms to replace the exhausted flame gases at the measured flow rate and a temperature of 350 °C (based on thermocouple measurements). Together this suggests a cycling time of 8.8 ms and hence a baseline frequency of 113 Hz. This value agrees very well with experimentally observed baseline frequencies. While the calculation here is somewhat crude and several factors have not been considered, it is clear that the proposed mechanism yields reasonable estimates of the frequencies observed for the AFD. In addition, all of the observations made thus far are consistent with this mechanism of oscillatory chemical kinetics.

When a hydrocarbon analyte is introduced into the premixed flame, the burning velocity decreases, and the flame front is not expected to travel as far into the capillary as under baseline conditions (this view is supported by visual observations of the flame). Consequently, the shorter exhausted premix column is replenished faster, and the frequency of cycling increases, signaling the presence of analyte through a change in acoustic pitch.

This scenario is again qualitatively consistent with all observations. It does not, however, allow a calculation of the absolute frequency in the presence of analyte. The changes in frequency introduced by analyte in this work are larger than one might expect on the basis of related studies of burning velocities.[19] This should come as no surprise since oscillating chemical systems are, so to speak, on the edge of extinction. As such, small differences in conditions can lead to large differences in behavior. This is, after all, what makes these systems analytically so useful and mechanistically so difficult. In the present case, too little is known about the transient interplay of gas-phase reactions within the system to suggest a detailed mechanistic interpretation. Relationships among factors such as temperature, surface reactions, hydrocarbon degradation products, flame propagating and terminating species, flame front composition, burning velocities, and quenching diameters are likely to be very complex. Indeed, the AFD may be able to shed some light on these aspects of flame chemistry in future studies. In this work, however, an exploration of the analytical characteristics of the AFD takes precedence.

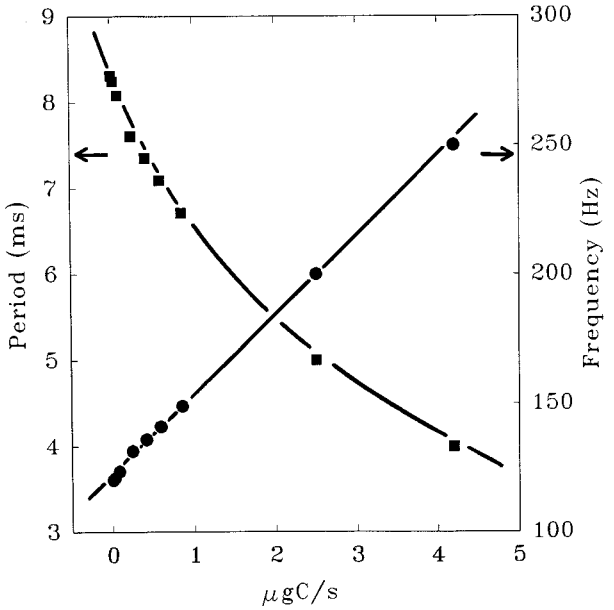

Figure 5. Working curves for *n*-dodecane using period and frequency of acoustic bursts as the response variables.

Analytical Response. With the basic response mechanism of the AFD thus established, this study could proceed to examine analytical characteristics of the detector. Initial investigations were carried out to determine whether the parameter to be measured should be the change in frequency, Δf, or the change in period, ΔT. Since the the frequency change in oscillations is substantial compared to the baseline, these measurements are not equivalent. Working curves for *n*-dodecane are shown in Figure 5 for both response parameters and indicate substantially better linearity in the frequency domain. This characteristic may have mechanistic implications but was not further examined. For the purpose of analytical characterization, additional studies reported here employed Δf as the response variable.

The response of the AFD is linear over about 3 orders of magnitude, as shown in Figure 6 for *n*-dodecane. The response is measured as the peak height (maximum frequency shift) for the analyte. The upper end of the linear range is determined by the point at which oscillations terminate due to overloading by the analyte; the lower end is determined by the level of baseline noise. A signal approaching the current limits of detection is shown in Figure 7. Because points are acquired at intervals of about 10 ms, there is extensive opportunity to perform digital filtering, and in this case a 111-point moving average filter has been applied to the data with little apparent distortion to the peak. Strictly speaking, the application of a digital filter of this type requires points to be evenly spaced, whereas in this case the interval between points varies with the frequency of the oscillations. Nevertheless, the interval is consistent enough to make this approach effective.

Fourier transforms of the baseline signal revealed that the dominant noise contributions were at low frequencies, particularly below 1 Hz. This is consistent with the frequency characteristics of flame flicker ($1/f$) noise in optical emission measurements, and the noise probably arises from similar processes (fluctuations in gas flow, drafts, etc.). There was also a small component of quantization noise from the limited resolution of the frequency measurement, but this can be easily remedied through filtering or an increase in the reference frequency. The minimum

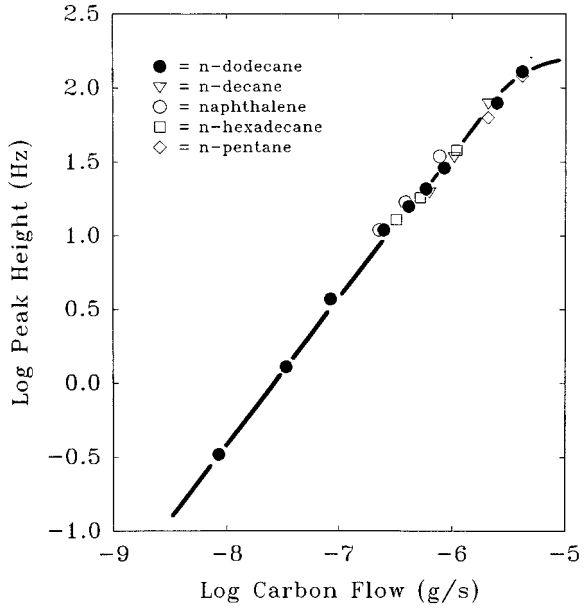

Figure 6. Response characteristics for several hydrocarbons. The solid line has a slope of unity.

Figure 7. Acoustochromatogram for 100 ng of *n*-dodecane (isothermal run, 200 °C).

detectable limit under current operating conditions is estimated to be 1−5 ng C/s. This is 2−3 orders of magnitude worse than a good FID response but compares well with that of a thermal conductivity detector and is very impressive compared to limits obtainable with other acoustic detection methods that have been developed. Improvements in this limit of detection are likely with the use of optimum digital filtering techniques and refinements to the apparatus (more careful regulation of gas flows, exclusion of drafts, etc.).

The AFD appears to be a mass-sensitive detector, and different peak profiles for the same amount of injected analyte were found to produce approximately the same area. Most analytes gave rise to a tail, which is likely due to a lag in the detector's recovery, but the precise reason for this is unknown. Several different burner geometries and operating conditions were investigated in an attempt to optimize the sensitivity of the AFD. It was found that every condition that yielded an analyte response, regardless of gas composition, burner diameter or shape, or flow rate, gave approximately the same change in frequency for a given amount of analyte. At most, a 2- or 3-fold improvement was observed for

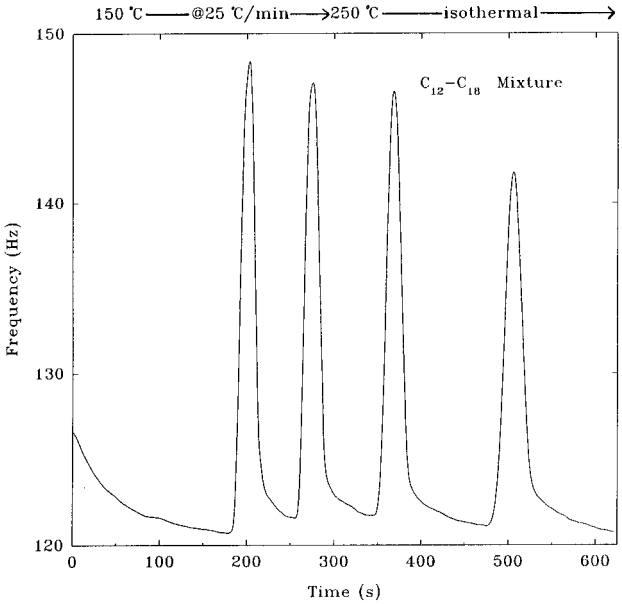

Figure 8. Acoustochromatogram for a series of *n*-alkanes. Temperature-programmed conditions are indicated at the top of the figure.

smaller flow rates, but this was obtained at the expense of a more limited range. The best compromise seemed to be obtained somewhere in the middle of the operational region. An increase in the flow rate of premix air was found to decrease the baseline frequency of the AFD and, at the limit, resulted in a loss of oscillation and eventual establishment of a reactive flow within the capillary. In contrast, an increase in auxiliary air brought about an increase in the baseline frequency. Different burner diameters led to different flow and frequency ranges for operation. This is presumably related to different quenching diameters of the flame front. When the inside of the end of the capillary was made conical (apex down) rather than flat, the flame was observed to descend partially into the cone and find a preferred position there. With this type of burner, the flame operates on a variable diameter, and the range of oscillatory stability is extended. It is interesting to note that, at certain cone angles, the response characteristics are inverted and presence of analyte leads to a decrease in frequency. Peaks were also found to have a more rounded shape with this burner geometry. Finally, several different gas compositions were employed to investigate the generality of the singing flame phenomenon. Other combustible mixtures, such as H_2/O_2 and CH_4/O_2, were also observed to yield acoustically active flames. While some differences in the characteristics of these flames were observed, none of the modifications led to significant improvements in response.

An acoustochromatogram of a series of four hydrocarbons is shown in Figure 8. Like the FID, the AFD appears to be immune to the effects of temperature programming. The response seems to be consistently linear for a number of hydrocarbons, as shown in Figure 6, with only minor changes in sensitivity for these compounds. There seems to be little discrimination among different types of combustible carbon (i.e., different molecular structures) by the AFD. A cursory investigation of the sensitivity of the detector for a variety of compounds was conducted, and the results are reported in Table 1. As shown in Figure 9, the molar response seems to correlate fairly well with the number of carbon atoms, as one might expect from other similarities with the FID. The concept of an "effective carbon number" that has

Table 1. Sensitivity of the AFD to Various Compounds

compound	response (Hz·s/μg)	response (Hz·s/nmol)
(A) *n*-hexadecane	30	6.9
(B) *n*-dodecane	27	4.9
(C) *n*-decane	24	3.4
(D) naphthalene	41	5.2
(E) *n*-pentane	25	1.8
(F) cyclohexanone	13	1.2
(G) cyclohexanol	13	1.3
(H) pyridine	15	1.2
(I) pyrazine	20	1.6
(J) ethyl decanoate	24	4.8
(K) *p*-methylbenzophenone	25	4.9
(L) 1,3,5-trioxane	7.5	0.68
(M) 1,2,3-trichlorobenzene	8.3	1.5
(N) *o*-iodotoluene	18	3.8
(O) carbon tetrachloride	1.4	0.21
(P) thianaphthene	20	2.7
(Q) carbon disulfide	9.1	0.69
(R) carbon dioxide	0.041	0.0018
(S) tetra-*n*-butyltin	180[a]	61[a]
(T) triethylphosphite	10	1.7
(U) tetraethyllead	18[a]	5.7[a]
(V) methylcyclopentadienyl-manganese tricarbonyl	100[a]	22[a]
(W) iron pentacarbonyl	20[a]	3.9[a]
nitric oxide	1.7	0.050
ammonia	2.4	0.040
air	−0.17	−0.0050
oxygen	−1.1	−0.035
hydrogen	−1.1	−0.0022
deuterium	−0.50	−0.0020
argon	−0.018	−0.00073
helium	−2.2	−0.0090
nitrogen	0	0

[a] Response was estimated in these cases, since the signal did not return to the baseline.

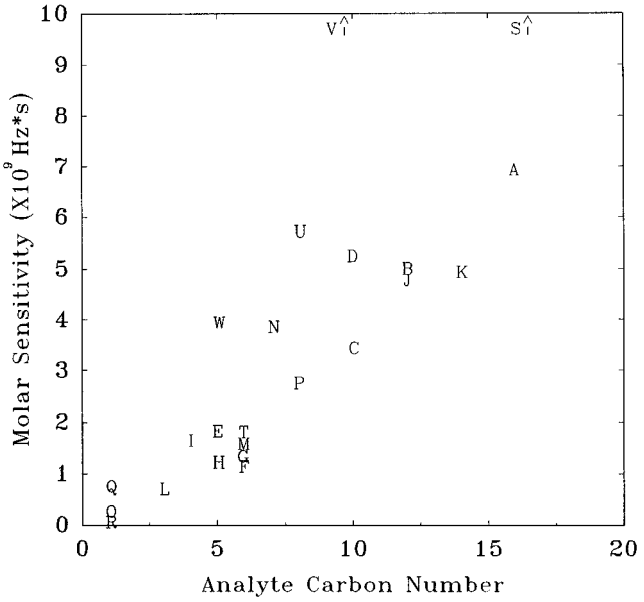

Figure 9. Molar sensitivity as a function of the number of carbon atoms in the analyte. Points are labeled in accordance with Table 1. Compounds S and V are off-scale and not shown.

been used in studying FID responses[3,22−26] may also be useful here, but the highly accurate measurements needed to verify this were not carried out.

The most interesting effect—and one not found in the FID to our knowledge—is the large positive response of certain compounds that can act as radical scavengers (for instance, in the role of antiknock additives or flame retarders). The responses for the tin and manganese compounds (but strangely not for the lead compound) were roughly an order of magnitude larger than those for a typical alkane and are not shown in Figure 9 because they are well off-scale. However, for tin-, lead-, manganese-, and iron-containing compounds, the signal failed to return to baseline for a long time after the peak signal, possibly due to deposition of the metal on the capillary rim, which is critical to the response. Earlier unpublished work in our laboratory has shown that a typical hydrogenation catalyst (e.g., Pt), when deposited inside the capillary, significantly altered the behavior of the reactive flow. Only a much more thorough investigation could clarify the possible involvement of surface effects and the nature of the enhanced response for Sn and Mn (and possibly other organometallic) compounds.

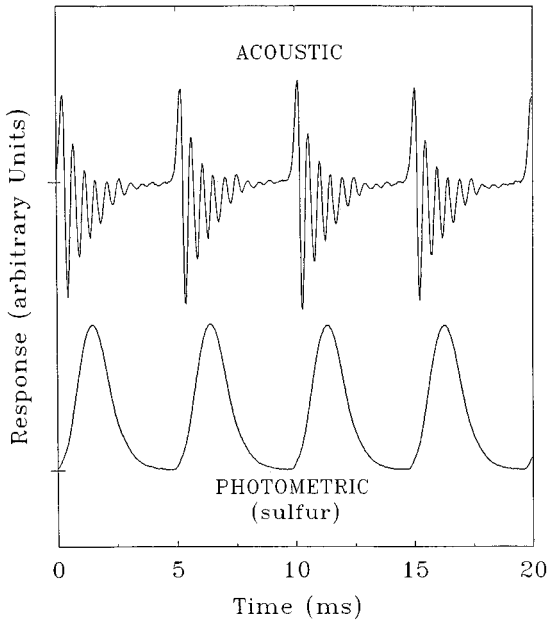

Figure 10. Time relationship between acoustic and photometric signals for sulfur.

With reference to other compounds listed in Table 1, there is no clear evidence that heteroatoms such as O, N, P, S, Cl, and I markedly influence response. As in the FID, there is no significant peak observed for carbon dioxide, and the signal for carbon tetrachloride is very low. The response of several non-carbon-containing gases is also very small and sometimes even negative (i.e., the peak is inverted and the oscillation frequency decreases).

One final interesting response characteristic was observed when the acoustic oscillations were compared with the flame photometric response of the detector to sulfur- and phosphorus-containing compounds. As shown in Figure 10, the peak of the photometric emission from sulfur lags the onset of the acoustic transient by about 2 ms. Similar results were observed for phosphorus, but the emission from carbon was coincident with the start of the acoustic pulse. The delayed responses for sulfur

(22) Bocek, P.; Janak, J. *Chromatogr. Rev.* **1971**, *15*, 111−150.
(23) Sternberg, J. C.; Gallaway, W. S.; Jones, D. T. L. *Gas Chromatography*; 3rd International Symposium, Instrument Society of America; Academic Press: New York, 1962; pp 231−267.
(24) Jorgensen, A. D.; Picel, K. C.; Stamoudis, V. C. *Anal. Chem.* **1990**, *62*, 683−689.
(25) Dressler, M.; Ciganek, M. *J. Chromatogr.* **1994**, *679*, 299−305.
(26) Blades, A. T. *J. Chromatogr. Sci.* **1984**, *22*, 120−121.

and phosphorus are consistent with literature results from a pulsed FPD system,[17,18] although there is a difference in the lag times. This raises the possibility of acoustically gated photometric detection, potentially leading to improved selectivity, but this mode of operation has yet to be examined.

CONCLUSIONS

This work demonstrated for the first time the use of passive acoustic detection in chromatography. While not as sensitive as some other chromatographic detectors, the AFD is within the range of practical utility and possibly amenable to future improvement. Most of its qualitative response characteristics are similar to those of the FID. An enhanced response for some metal-containing compounds was found but was accompanied by excessive tailing. The AFD may also be useful in obtaining a better understanding of the dynamics of flame chemistry. While the AFD is inexpensive and easy to construct, further investigations will be needed to determine whether it exhibits sound advantages relative to conventional GC detectors, or whether it will remain an oddity like so many other detectors that have been developed over the years.

ACKNOWLEDGMENT

The authors gratefully acknowledge the assistance of Chris Turner for his contributions to software development and of Dr. R. Stephens for his many helpful suggestions. D. Abriel is acknowledged for his photographic expertise. This work was supported by the Natural Sciences and Engineering Research Council (NSERC) of Canada.

Received for review December 29, 1995. Accepted May 14, 1996.[⊗]

AC951243Q

[⊗] Abstract published in *Advance ACS Abstracts,* June 15, 1996.